

Spin fluctuations and superconductivity in layered f -electron superlattices

Yasuhiro Tada^{1,*} and Robert Peters²

¹*Institute for Solid State Physics, The University of Tokyo, Kashiwa 277-8581, Japan*

²*Computational Condensed Matter Physics Laboratory, RIKEN, Wako, Saitama 351-0198, Japan*

We investigate magnetic and superconducting properties of layered f -electron superlattices within the fluctuation exchange approximation (FLEX). We show that spin fluctuations, which are characterized by the maximum value of the spin susceptibility in the 3-dimensional (3D) Brillouin zone, are strongly suppressed in f -electron superlattices. However, effective 2D spin fluctuations can be increased due to the spatial confinement of the f -electrons. Therefore, the tendency towards $d_{x^2-y^2}$ -wave superconductivity, mediated by these spin fluctuations, can be strongly increased in f -electron-superlattices. This is in sharp contrast to superlattices composed of conventional s -wave superconductors, where superconductivity is generally suppressed.

PACS numbers:

I. INTRODUCTION

Recent experimental realizations of layered superlattices, $\text{CeIn}_3/\text{LaIn}_3$ and $\text{CeCoIn}_5/\text{YbCoIn}_5$, have opened new possibilities in the field of f -electron systems.¹⁻⁴ Due to a non-trivial interplay of strong correlations and tunable dimensionality, novel phenomena have been observed in these f -electron superlattices which have not been seen so far in existing magnetic/superconducting superlattices composed of weakly or non-interacting systems.⁵⁻¹⁴

For example, it has been found that magnetic properties of $\text{CeIn}_3(n)/\text{LaIn}_3(4)$ superlattices¹ depend on the thickness of the CeIn_3 -layer within the unit cell of the superlattice. In bulk CeIn_3 , the coherence temperature is $T_{\text{coh}} \sim 50(\text{K})$ and the Néel temperature is $T_N \simeq 10(\text{K})$ with an ordering vector $\mathbf{Q} = (\pi, \pi, \pi)$.¹⁵⁻¹⁷ Remarkably, it has been reported that the Néel temperature of the superlattice is suppressed when the width of the CeIn_3 -layers, n , is reduced, and eventually approaches zero for $n = 2$. At the same time, a linear temperature dependence in the in-plane resistivity is observed for $n = 2$, suggesting that the dimensionality of the antiferromagnetic (AF) spin fluctuations is reduced from 3-dimensions in bulk CeIn_3 to 2-dimensions in the superlattice. Such an anomalous behavior in the resistivity has never been observed in previous studies of magnetic superlattices, and would be characteristic for f -electron superlattices.

Furthermore, superconductivity in $\text{CeCoIn}_5/\text{YbCoIn}_5$ superlattices has been investigated.²⁻⁴ In bulk CeCoIn_5 , the coherence temperature is $T_{\text{coh}} \sim 50(\text{K})$ and the superconducting transition temperature is $T_c \sim 2.3(\text{K})$.^{17,18} CeCoIn_5 is located near an AF quantum critical point and AF spin fluctuations are expected to be important for the normal state as well as for superconductivity. In the bulk system, the AF spin fluctuations are especially strong around $\mathbf{Q} = (\pi, \pi, \pi)$ due to the nesting of the Fermi surface, and they can be characterized as 3D-like.¹⁹⁻²¹ It is generally considered that the superconductivity exhibits $d_{x^2-y^2}$ -wave symmetry and is mediated by these AF spin fluctuations. Experiments on $\text{CeCoIn}_5/\text{YbCoIn}_5$ superlattices have demonstrated that

superconductivity exists even for thin CeCoIn_5 -layers and that the superconducting transition temperature, T_c , is suppressed as the width of the CeCoIn_5 -layers in the unit cell is reduced. However, it must be noted that at the same time effects of disorder, which are estimated from the residual resistivity, are increased in thin CeCoIn_5 -layers. It is thus unclear, how the superconductivity behaves in “clean” f -electron superlattices.

Motivated by these experiments, there have been several theoretical studies. The effects of a possible Rashba-like spin-orbit coupling due to local inversion symmetry breaking near the interfaces of the Ce-layers and the spacer layers²²⁻²⁵ have been investigated. When the Rashba-like interaction is sufficiently large, the Pauli depairing effect is greatly suppressed and novel superconducting states might be stabilized when a magnetic field is applied. In another theoretical study, the experimental data was analyzed based on the Berezinskii-Kosterlitz-Thouless transition by regarding the superlattice as a junction composed of a normal metal and a superconductor.²⁶ If this junction picture is applicable to the f -electron superlattice, then superconductivity in the YbCoIn_5 -layer would be strongly suppressed, because of a large mismatch between the Fermi velocities of the CeCoIn_5 -layer and the YbCoIn_5 -layer, leading to a 2-dimensional superconductivity in the CeCoIn_5 -layers.

In these previous studies neither electron correlations nor the superlattice structure are explicitly considered. However, these are two key ingredients in f -electron superlattices and distinguish them from all the existing non-interacting superlattices and the bulk f -electron compounds. To understand f -electron superlattices, it is necessary to clarify the impact of electron correlations and the superlattice structure, and also their possible interplay. In two previous studies, the present authors already discussed the Kondo effect and quasi-particles properties^{27,28} using the dynamical mean field theory (DMFT), which captures local strong correlations, but neglects non-local fluctuations. This time, we analyze magnetic and superconducting properties of f -electron superlattices using the fluctuation exchange approximation (FLEX) in order to describe spatially extended spin

fluctuations.²⁹ We use a periodic Anderson model (PAM) which is defined on a superlattice. This model can be considered as a minimal model to describe f -electron superlattices, because it takes into account both the electron correlations and the superlattice structures.

This paper is organized as follows: In Sec. II, we introduce our model, the FLEX approximation for the spin fluctuations, and the Eliashberg equations for the superconductivity. Spin fluctuations are discussed in Sec. III, and the superconducting instability is examined in Sec. IV. Finally, in Sec. V we shortly summarize this paper.

II. MODEL

Because the f -electrons in the Yb-sites form a closed shell, the YbCoIn₅-layers in CeCoIn₅/YbCoIn₅ superlattices can be treated as normal uncorrelated metals. Indeed, the resistivity in bulk YbCoIn₅ shows a monotonic temperature dependence without any signature of the Kondo effect. Similarly, in the CeIn₃/LaIn₃ superlattices, only the CeIn₃-layers provide f -electrons at the Fermi energy. Therefore, both superlattices can be considered as heterostructure composed of layers including f -electrons and layers without. In order to understand these f -electron superlattices, we introduce a PAM which consists of two kinds of layers, henceforth called “A-layers” and “B-layers”. The A-layers include conduction electrons (c -electrons) and f -electrons, which corresponds to CeIn₃- or CeCoIn₅-layers, while within the B-layers only c -electrons exist, which corresponds to the LaIn₃- and YbCoIn₅-layers. Our Hamiltonian thus reads

$$H = - \sum_{rr'\sigma} t_{rr'}^c c_{r\sigma}^\dagger c_{r'\sigma} - \sum_{rr' \in A, \sigma} t_{rr'}^f f_{r\sigma}^\dagger f_{r'\sigma} - \mu \sum_{r\sigma} c_{r\sigma}^\dagger c_{r\sigma} - (\mu - \epsilon^f) \sum_{r \in A, \sigma} f_{r\sigma}^\dagger f_{r\sigma} + V \sum_{r \in A, \sigma} [c_{r\sigma}^\dagger f_{r\sigma} + f_{r\sigma}^\dagger c_{r\sigma}] + U \sum_{r \in A} n_{r\uparrow}^f n_{r\downarrow}^f, \quad (1)$$

where $c_{r\sigma}$ and $f_{r\sigma}$ are annihilation operators for the conduction electrons and the f -electrons, respectively. $r = (r_\parallel, z) = (x, y, z)$ is a site index which is composed of an in-plane index r_\parallel , and a layer index z . σ corresponds to the spin index. Each layer forms a square lattice, and hopping is only allowed between nearest neighbor sites for simplicity; $t_{r_\parallel z r'_\parallel z}^a = t_1^a$ for $r_\parallel \neq r'_\parallel$ and $t_{r_\parallel z r_\parallel z'}^a = t_2^a$ for $z \neq z'$ where $a = c, f$. The number of A-layers and B-layers within the unit cell of the superlattice are given by L_A and L_B . In the present study, we fix $L_A = 1$ for which effects of the spatial confinement of the f -electrons are expected to be particularly strong. Because of $t_2^f = 0$ and the absence of a direct hopping between the A-layers, which are separated by the B-layers, the f -electrons can move along the z -direction only through the B-layers. The model parameters are chosen as $(t_1^c, V, \epsilon_f) = (5.0, 2.0, 0)$ and the total filling is

fixed to $n = n^c + n^f = 0.95$, which are a reasonable set of parameters and similar to the ones used in the previous DMFT study.²⁷ The interaction strength is fixed at a moderate value, $U = 3.0$, for which a clear divergence in the spin susceptibility of the 3D system ($L_B = 0$) is visible at low temperature. The z -axis hopping t_2^c characterizes an anisotropy of the system for $L_B = 0$.

In order to analyze momentum-resolved properties, we perform a Fourier transform,

$$c_{jz\sigma} = \sum_{k_\parallel k_z l} U_{j\tilde{z}_1 \tilde{z}_2, k_\parallel k_z l}^c c_{k_\parallel k_z l \sigma}, \quad (2)$$

$$f_{jz\sigma} = \sum_{k_\parallel k_z} U_{j\tilde{z}_1 \tilde{z}_2, k_\parallel k_z}^f f_{k_\parallel k_z \sigma}, \quad (3)$$

where the unitary matrices U^c and U^f are defined as,

$$U_{j\tilde{z}_1 \tilde{z}_2, k_\parallel k_z l}^c = \frac{e^{ik_\parallel r_\parallel}}{\sqrt{N_\parallel}} \frac{e^{ik_z z + iq_l^c \tilde{z}_2}}{\sqrt{N_z}}, \quad (4)$$

$$U_{j\tilde{z}_1 \tilde{z}_2, k_\parallel k_z}^f = \frac{e^{ik_\parallel r_\parallel}}{\sqrt{N_\parallel}} \frac{e^{ik_z z}}{\sqrt{N_z/L}}, \quad (5)$$

$\mathbf{k}_\parallel = (k_x, k_y)$. The layer index z is parametrized as $z = L\tilde{z}_1 + \tilde{z}_2$ with $0 \leq \tilde{z}_2 < L$ for U^c and $\tilde{z}_2 = 1$ for U^f , and $0 \leq l < L$ for U^c , $q_l^c = 2\pi l/L$. The momentum along the z -axis is defined within the reduced Brillouin zone (RBZ), $0 \leq k_z < 2\pi/L$. N_\parallel is the total number of sites within a layer and N_z is the total number of layers. Thus, the total number of sites is given by $N = N_\parallel N_z$.

In FLEX, we focus on spatially extended spin fluctuations.²⁹ The selfenergy and susceptibilities in the normal state are given by,

$$\Sigma^f(k) = \frac{T}{N} \sum_q V^f(q) G^f(k-q), \quad (6)$$

$$V^f(q) = \frac{1}{2} U^2 \chi_c^f(q) + \frac{3}{2} U^2 \chi_s^f(q) - U^2 \chi_0^f(q) \quad (7)$$

$$\chi_0^f(q) = -\frac{T}{N} \sum_q G^f(k+q) G^f(k), \quad (8)$$

$$\chi_c^f(q) = \frac{\chi_0^f(q)}{1 + U \chi_0^f(q)}, \quad (9)$$

$$\chi_s^f(q) = \frac{\chi_0^f(q)}{1 - U \chi_0^f(q)}, \quad (10)$$

where $k = (i\omega_n, \mathbf{k})$ with $\mathbf{k} = (\mathbf{k}_\parallel, k_z)$. $G^f(k)$ is the f -electron Green's function in the $f_{k\sigma}$ -basis. Note that the f -electron contributions to the total spin susceptibility are dominant, especially near magnetic criticality, and that they are strongly enhanced by the interaction U . On the other hand, contributions from the c -electrons are not enhanced by an interaction term in the present model.

The superconducting instability is investigated within the linearized Eliashberg equation for the singlet gap

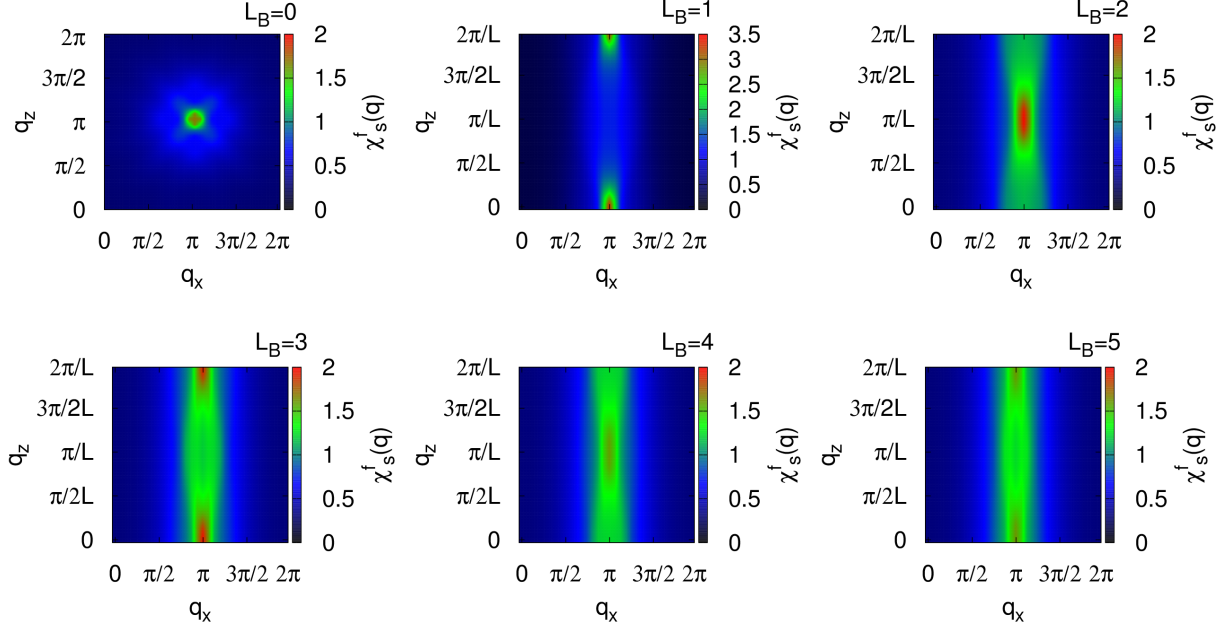


FIG. 1: Spin susceptibility $\chi_s^f(i\omega_n = 0, \mathbf{q})$ at $T = 0.1$ in the xz -plane at $q_y = \pi$ for $t_2^c = t_1^c$ for different L_B .

function $\Delta^f(k)$,

$$\Delta^f(k) = -\frac{T}{N} \sum_{k'} V_s^f(k - k') |G^f(k')|^2 \Delta^f(k'), \quad (11)$$

$$V_s^f(q) = U - \frac{1}{2} U^2 \chi_c^f(q) + \frac{3}{2} U^2 \chi_s^f(q). \quad (12)$$

It is noted that, c -electrons can only become superconducting via the f -electrons by the proximity effect, because of the absence of c -electrons interactions. The proximity effect is well taken into account in our calculations because the f -electron Green's function G^f fully includes the hybridization processes between the f -electrons and the c -electrons through V .

III. SPIN FLUCTUATIONS

In this section, we discuss the spin fluctuations as calculated by the FLEX. First, we consider an isotropic parameter set, $t_2^c = t_1^c$, where anisotropy between the xy - and z -directions can only originate from the superlattice structure when $L_B \geq 1$. Figure 1 shows the q -dependence of the magnetic susceptibility, $\chi_s^f(i\omega_n = 0, \mathbf{q})$, at relatively high temperature, $T = 0.1$. The positions of the maximum values of χ_s^f oscillate depending on the number of spacer layers L_B . When L_B is even, the maximum values are located at $\mathbf{Q} = (\pi, \pi, \pi/L)$; when L_B is odd they are at $\mathbf{Q} = (\pi, \pi, 0)$. These momenta correspond to the spin configurations shown in Fig. 2. When L_B is odd (even), the magnetic coupling between different A-layers, which is mediated by the c -electrons, is

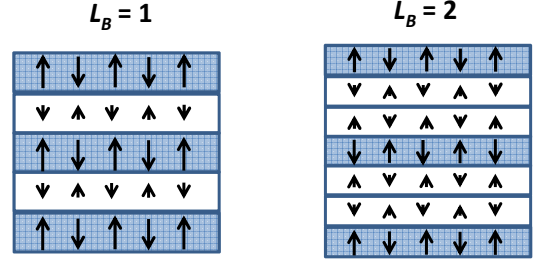


FIG. 2: Schematic picture of the spin configurations for $L_B = 1$ (left panel) and $L_B = 2$ (right panel). Shaded layers and white layers are A-layers and B-layers, respectively.

ferromagnetic (antiferromagnetic). Due to the proximity to the A-layers, small moments are induced into the spacer B-layers in a consistent way with the magnetic structures of the A-layers. Similar oscillating inter-layer magnetic structures and induced moments have been found in DMFT calculations, which support the present FLEX study.³⁰ Furthermore, such oscillations in the magnetic inter-layer coupling have also been commonly found in ferromagnetic superlattices.^{10–12} One intuitive understanding of this phenomena is based on the RKKY interaction between magnetic layers separated by metallic spacer layers.^{13,14} The magnetic inter-layer coupling is asymptotically given by $\sim J \sin 2k_F z / z^2$ with the Fermi wavenumber k_F and coupling strength J . In the present study, the system is close to half filling so that the Fermi wavenumber of the c -electrons at $V = 0$ along the z -axis is $\sim \pi/2$, which leads to the above-mentioned periodicity

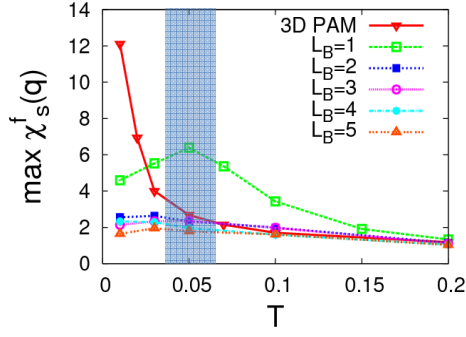


FIG. 3: Temperature dependence of the maximum value of $\chi_s^f(i\omega_n = 0, \mathbf{q})$ for $t_2^c = t_1^c$. Shaded region indicates the characteristic temperature scale T_0 .

in $\chi_s^f(q)$.

We can estimate the strength of the spin fluctuations by the maximum value $\chi_s^f(i\omega_n = 0, \mathbf{Q})$, which we show in Fig. 3. We want to note here, that the magnitude of this maximum value is strongly parameter dependent, because already small changes in the density of states can lead to a substantial enhancement of the Stoner factor (Eq. 10), if the system is close to magnetic criticality. A general behavior observed in our calculations is that the susceptibility χ_s^f for the 3D bulk system (without superlattice structure, $L_B = 0$) strongly increases below a characteristic temperature T_0 , indicated by the shaded region in the figure, $T_0 \sim 0.05$. At the same temperature, the single peak in χ_s^f , which is present at high temperature (Fig. 1), is split as shown in Fig. 4. Due to the hybridization between c - and f -electrons, the Fermi surface is split and the nesting properties are changed at low temperatures as seen in Fig. 5. Thus, the spin fluctuations are strongly affected by V for $T < T_0$ where heavy fermions with long lifetime are well formed within the present FLEX calculations.

In the f -electron superlattice, $L_B \neq 0$, the Fermi surface differs strongly from the 3D bulk system.²⁷ Particularly, a q_z -dependence of $\chi_s^f(q)$ arises only from t_2^c through V , because a direct hopping between different A-layers separated by the spacer B-layers is forbidden in the present model. A general behavior observed for the superlattice is that, similar to the bulk system, the single peak in the susceptibility at high temperature is split into four peaks at low temperatures, $T < T_0 \sim 0.05$, as shown in Fig. 4. However, the abrupt increase in the susceptibility, which is observed in the bulk system at low temperature, is cut off in the superlattice around T_0 and the susceptibility decreases for $T < T_0$, as shown in Fig. 3. While at high temperature, $T > T_0$, the Fermi surface is mainly determined by the c -electrons, below T_0 the f -electrons and thus the superlattice structure become important. As a consequence, for temperatures below T_0 the nesting of the Fermi surface in the superlattice is changed and $\mathbf{Q} \sim (\pi, \pi, \pi)$ is no longer a good nesting vector as can be seen in Fig. 5. Therefore, as T is

decreased and the Fermi surface becomes affected by the superlattice structure through V , the lack of good nesting properties of the Fermi surface cuts off the enhancement of the spin fluctuations. We note that the large value of $\max[\chi_s^f]$ for $L_B = 1$ originates in a large density of states near the Fermi energy due to the superlattice structure²⁸ which leads to a substantial enhancement in the Stoner factor, as mentioned above. However, while this strong enhancement at finite temperature for $L_B = 1$ is strongly parameter dependent, the decrease of the susceptibility in the superlattice below T_0 has been observed for a wide range of the parameters.

As shown in Fig. 4, spin fluctuations in the superlattice are smeared out at low temperatures within the q_z direction. The q_z -dependence of $\chi_s^f(q)$ becomes weaker as L_B is increased. Thus, spin fluctuations become more 2-dimensional-like when L_B is increased. However, this also means that the peak height of $\chi_s^f(q)$ in the 3D Brillouin zone is not an appropriate measure for the strength of the spin fluctuations when L_B is large. In order to estimate the strength of the spin fluctuations, we consider an effective 2D spin susceptibility

$$\chi_{s2D}^f(i\omega_n, \mathbf{q}_{\parallel}) = \frac{1}{N_z} \sum_{q_z} \chi_s^f(i\omega_n, \mathbf{q}). \quad (13)$$

$\chi_{s2D}^f(q_{\parallel})$ has its maximum at $\mathbf{Q}_{\parallel} \sim (\pi, \pi)$ for any L_B in the present model. We show the temperature dependence of the maximum values of $\chi_{s2D}^f(q_{\parallel})$ in Fig. 6. Although $\max[\chi_{s2D}^f]$ in the superlattice ($L_B \geq 1$) does not show a divergence at low temperature, this effective 2D spin susceptibility is clearly enhanced compared to the 3D PAM ($L_B = 0$) for the calculated temperature range. We note that the change in dimensionality of the spin fluctuations from 3D to 2D has also been experimentally observed in the CeIn₃/LaIn₃ superlattice as the CeIn₃-layer thickness (L_A in our model) was tuned with a fixed LaIn₃-layer thickness (L_B).¹ Although we cannot directly compare our results to the experiments, the suppression of the magnetic order in the superlattice and the calculated 2D-like character of the spin fluctuations are consistent with the experiments.

Up to now, we have analyzed the magnetic susceptibility for an isotropic model. However, CeCoIn₅ exhibits a cylindrical Fermi surface²¹. In order to investigate effects of an anisotropy in the original 3D model, we consider a system with a more 2D-like set of hopping parameters, $t_2^c = 0.5t_1^c$. Similarly to the isotropic hopping parameter set, we observe even-odd oscillations of the peak positions when L_B is changed, as shown in Fig. 7. We show the temperature dependence of the maximum values of $\chi_s^f(T)$ within the 3D Brillouin zone in Fig. 8. The susceptibility of the 3D PAM ($L_B = 0$), $\max[\chi_s^f(T)]$, behaves again monotonically and rapidly grows at low temperature. Furthermore, any increase in $\max[\chi_s^f(T)]$ for the superlattice, $L_B > 0$, is again cut off at low temperatures. However, because of the anisotropic parameter set, the bulk system, $L_B = 0$, already includes strong 2D

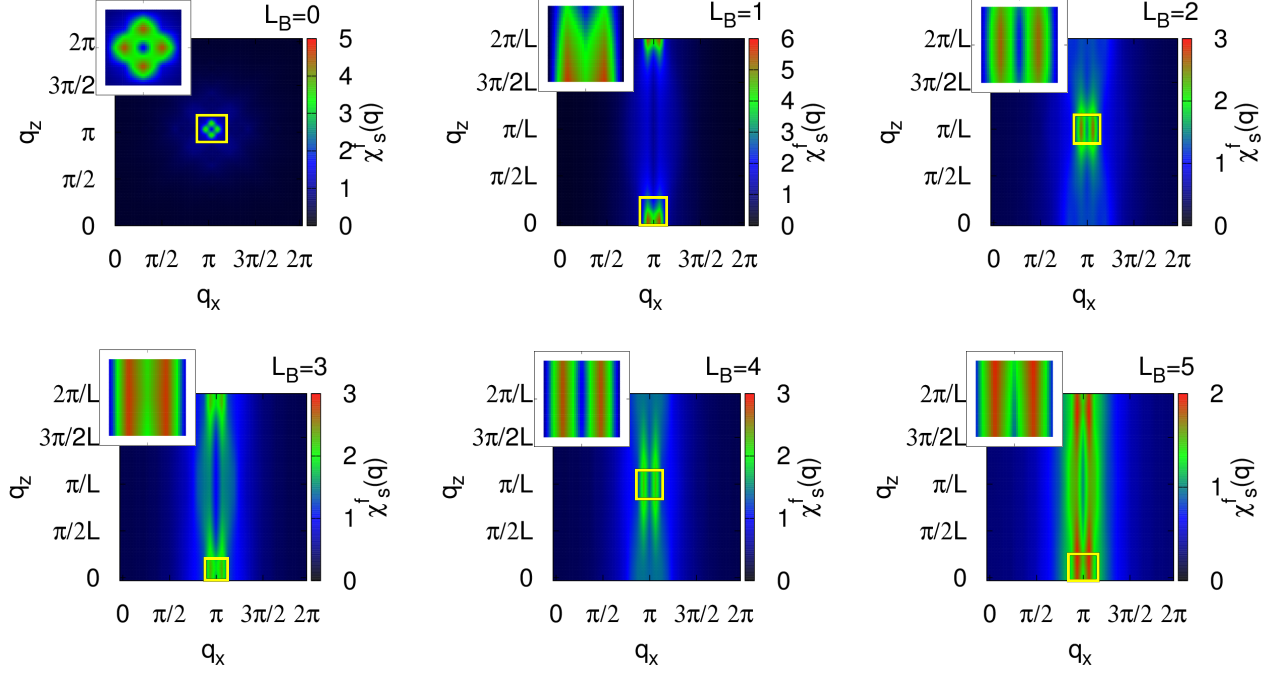


FIG. 4: Spin susceptibility $\chi_s^f(i\omega_n = 0, \mathbf{q})$ at $T = 0.03$ in the xz -plane at $q_y = \pi$ for $t_2^c = t_1^c$. The inset in each panel shows a magnification of the BZ as marked by the yellow square in the main plot.

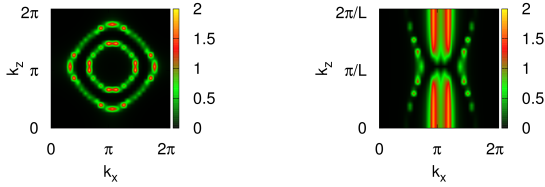


FIG. 5: Fermi surface as given by the spectral function $(-1/\pi)\text{Im}G^f(i\pi T, \mathbf{k})$ at a low temperature $T = 0.03$ with $k_y = 0$ for $L_B = 0$ (left panel) and $L_B = 1$ (right panel).

spin fluctuations, and the effective 2D spin susceptibility χ_{s2D}^f (not shown in the paper) is less enhanced in the superlattices. Comparing the results for the two parameter sets, $t_2^c = t_1^c$ and $t_2^c = 0.5t_1^c$, we find that the impact of the f -electron confinement to the A-layers is stronger when the hopping parameters are more 3-dimensional. This is reasonable, because in the limit of decoupled layers, $t_2^c \rightarrow 0$, the superlattice structure does not play a role at all. We have confirmed this tendency by performing similar calculations for different hopping parameters.

IV. SUPERCONDUCTIVITY

Finally, we investigate the impact of the increased 2D spin fluctuations in the superlattice on the superconductivity by solving the Eliashberg equation (11). First, in order to understand the proximity effect in our model, we consider s -wave superconductivity by replacing $V_s^f(q)$ in Eq. (11) by

$$V_{s\text{-wave}}^f(q) = -U_0\theta(\omega_D - |\omega_n|), \quad (14)$$

where we fix $\omega_D = 1.0$ and U_0 is tuned so that $\lambda = 1$ when $L_B = 0$ and $T = 0.02$. We then solve the Eliashberg equation without selfenergy. Thus, electron correlations are not included in this calculation. In Fig. 9, we show the maximum eigenvalues, $\max[\lambda]$, of the Eliashberg equation which corresponds to the strength of the superconducting instability. The largest eigenvalue, λ , rapidly decreases as L_B is increased, showing slight oscillations

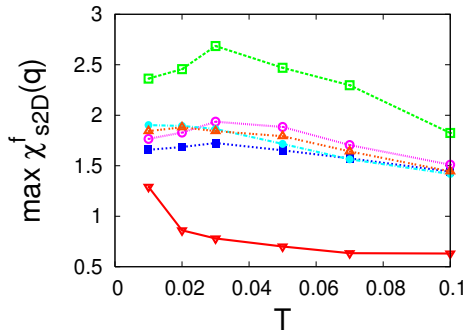


FIG. 6: Temperature dependence of the maximum value of $\chi_{s2D}^f(i\omega_n = 0, \mathbf{q}_{\parallel})$ for $t_2^c = t_1^c$. Symbols are the same as in Fig. 3

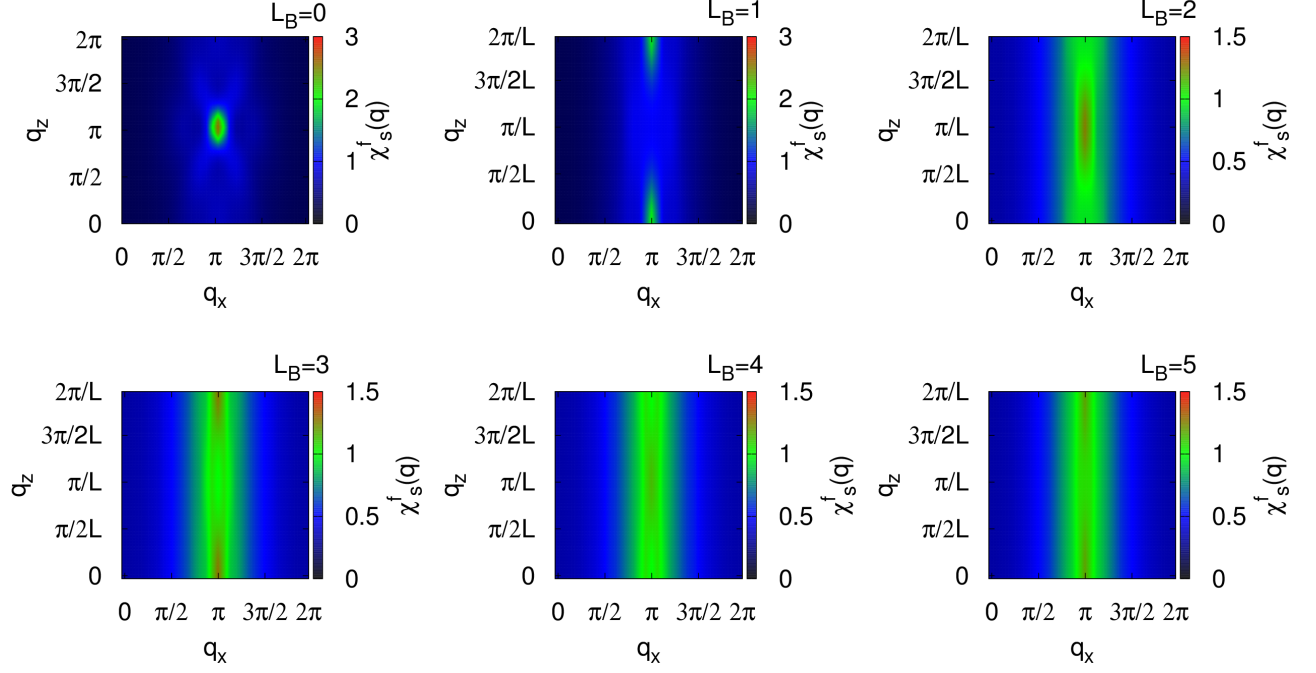


FIG. 7: Spin susceptibility $\chi_s^f(i\omega_n = 0, \mathbf{q})$ at $T = 0.1$ in the xz -plane at $q_y = \pi$ for $t_2^c = 0.5t_1^c$.

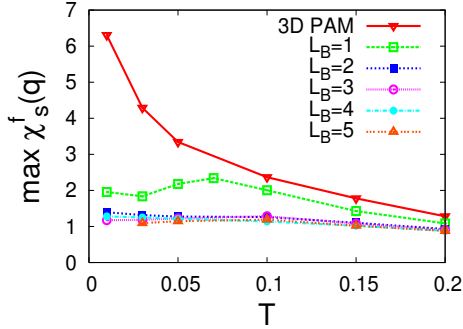


FIG. 8: Temperature dependence of the maximum value of $\chi_s^f(i\omega_n = 0, \mathbf{q})$ for $t_2^c = 0.5t_1^c$.

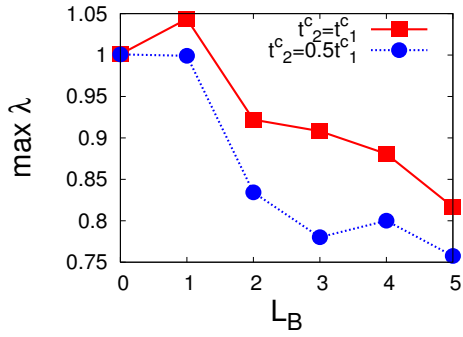


FIG. 9: Maximum eigenvalue λ for the s -wave superconductivity at fixed $T = 0.02$.

due to changes in the density of states at the Fermi energy which depend on the details of the model parameters. Thus, if conventional s -wave superconductivity, mediated by phonons, were realized in CeCoIn₅/YbCoIn₅ superlattices, one can expect that T_c is strongly decreased in the superlattice. Such a suppression of the superconductivity has been commonly observed in superlattices composed of s -wave superconductors and normal metals.^{5–9} Experimentally, T_c is lower in all the previous conventional superlattices compared to the corresponding bulk systems. It has theoretically been shown that the superconducting transition temperature T_c is suppressed in an exponential way in layered systems when the thickness of the normal metal layer L_N is increased,^{31–34}

$$T_c(L_N) \simeq T_c(0) - \delta T_c \tanh(L_N/\xi_0), \quad (15)$$

where $\delta T_c \simeq (T_c(L_N)/T_c(\infty))(T_c(0) - T_c(\infty))$ and ξ_0 is effective coherence length. This suppression of T_c comes from the fact that the pairing interaction which exists only in the superconductor layer mediates superconductivity not only in the superconductor layer, but also in the normal metal layer. Since this is a general property of the proximity effect, one could naively expect a suppression of superconductivity also for d -wave states, which are mediated by the spin-fluctuations.

In order to examine this further, we solve the Eliashberg equation with the pairing interaction $V_s^f(q)$ corresponding to spin fluctuations and the normal self-energy for $t_2^c = t_1^c$. Contrary to the s -wave superconductivity, as seen in Fig. 10, the maximum eigenvalues for the $d_{x^2-y^2}$ -wave superconductivity mediated by the

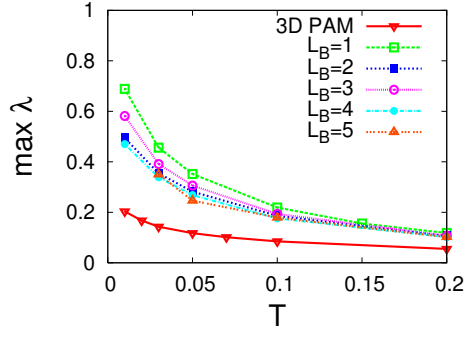


FIG. 10: The maximum eigenvalue of the Eliashberg equation for the $d_{x^2-y^2}$ -wave superconductivity when $t_2^c = t_1^c$.

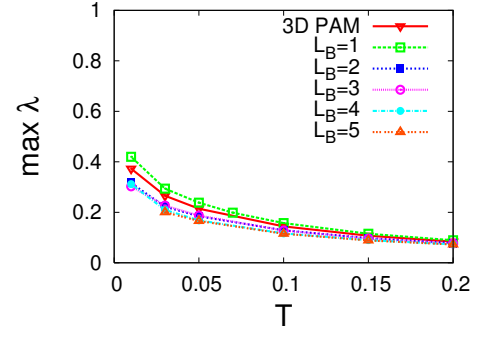


FIG. 12: The maximum eigenvalue of the Eliashberg equation for the $d_{x^2-y^2}$ -wave superconductivity when $t_2^c = 0.5t_1^c$.

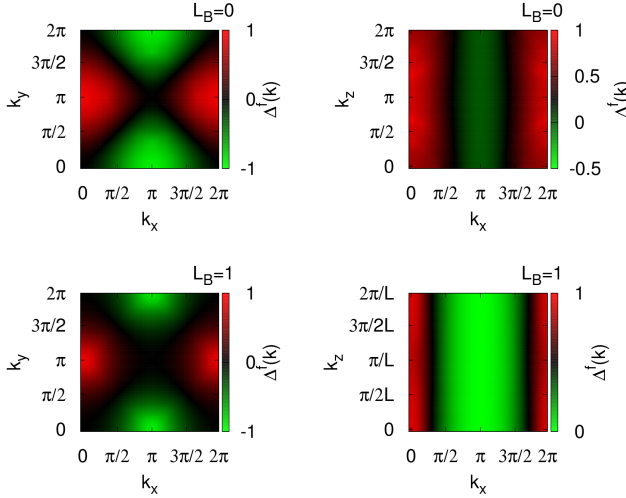


FIG. 11: Gap functions $\Delta(k_x, k_y, k_z = 0)$ and $\Delta(k_x, k_y = 0, k_z)$ at $\omega_n = \pi T$ for $L_B = 0, 1$ when $t_2^c = t_1^c$ and $T = 0.02$ in arbitrary units.

spin fluctuations are *enhanced* in the f -electron superlattices. Although the eigenvalues, $\max[\lambda]$, do not reach unity for the calculated temperature range, these results suggest that T_c for $d_{x^2-y^2}$ -wave superconductivity can be higher in the superlattice than in the bulk system. This strong d -wave superconducting instability in the f -electron superlattice can be understood by focusing on the effective 2D spin fluctuations discussed in the previous section. In order to stabilize the $d_{x^2-y^2}$ -wave superconductivity with $\Delta(k) \propto (\cos k_x - \cos k_y)$, the q_z -dependence in $V_s^f(q)$ is irrelevant and we only need to consider the $q_x q_y$ -dependence. As exemplified in Fig. 11, typical profiles of the $d_{x^2-y^2}$ -wave gap functions are indeed $\Delta(k) \sim (\cos k_x - \cos k_y)$ and their k_z -dependence is weak for any L_B . If we neglect the k_z -dependence in

$|G^f(k)|^2$, the Eliashberg equation is reduced to

$$\Delta^f(k_{\parallel}) \simeq -\frac{T}{N_{\parallel}} \sum_{k'_{\parallel}} V_{s2D}^f(k_{\parallel} - k'_{\parallel}) |G^f(k'_{\parallel})|^2 \Delta^f(k'_{\parallel}), \quad (16)$$

$$V_{s2D}^f(q_{\parallel}) = \frac{1}{N_z} \sum_{q_z} V_s^f(q). \quad (17)$$

From this equation, it is clear that the most important part of the pairing interaction is determined by $\chi_{s2D}^f(q_{\parallel})$ which is enhanced in the superlattice (Fig. 6). This enhancement of the effective pairing interaction can lead to an increased T_c , which is a consequence of the interplay between strong interaction among the f -electrons and the confinement of them within the superlattice structure. This is characteristic for the f -electron superlattice. We note that a similar enhancement of superconductivity has been theoretically found in 3D bulk models when tuning the hopping parameter in the z -direction^{35,36}. However, in these studies the proximity effect does not play a role. In our present study, superconductivity is enhanced as a result of a subtle interplay between the proximity effect and an increase of spin fluctuations in the superlattice.

Results for $\max[\lambda]$ when $t_2^c = 0.5t_1^c$ are shown in Fig. 12. For this parameter set the enhancement of χ_{s2D}^f in the superlattice is weak. Therefore, also the maximum eigenvalue of the Eliashberg equation are only slightly increased in the superlattice. T_c in the superlattice would be similar to the bulk value when the hopping parameters are 2D-like. However, the enhancement of χ_{s2D}^f in the superlattice due to the f -electron confinement is still important for these parameters. It almost cancels the suppression of d -wave superconductivity due to the proximity effect. Therefore, T_c in the superlattice can remain as high as in the bulk ($L_B = 0$) even for large L_B .

Experimentally it has been observed that T_c is lower in the CeCoIn₅/YbCoIn₅ superlattice than in bulk CeCoIn₅ with $T_c \simeq 2.3$ (K). We think that this can be explained by two reasons: First, the Fermi surface of CeCoIn₅ is cylindrical²¹ and thus would be better described by the

anisotropic parameter set in our calculations. Second, disorder effects seem to be strong for thin CeCoIn₅-layer superlattices.² In the experiments, the thickness of the YbCoIn₅-layers has been fixed and the number of the CeCoIn₅-layers has been tuned. We expect that if the thickness of the YbCoIn₅-layer is changed with a fixed CeCoIn₅-layer width, the behavior of T_c will deviates from conventional normal-metal/superconductor superlattices.

V. SUMMARY

We have investigated the f -electron superlattice based on FLEX. We found that the nature of the spin fluctuations is modified by the superlattice structure and the Q -vectors corresponding to the maximum in the susceptibility depend on the width of the spacer layers, similar to conventional magnetic superlattices. While the strength of the 3D spin fluctuations, characterized by $\max[\chi_s^f(q)]$

in the 3D Brillouin zone, is suppressed in the superlattice because good nesting properties of the Fermi surface are lost, effective 2D fluctuations are enhanced because of reduced dimensionality. These enhanced spin fluctuations can lead to higher T_c in the case of $d_{x^2-y^2}$ -wave superconductivity in the superlattice than in the bulk compounds, which is in sharp contrast to all the conventional superlattice superconductors. We hope that these results will lead to further experiments analyzing T_c in clean f -electron superlattices.

ACKNOWLEDGEMENT

We thank Y. Matsuda, T. Shibauchi, H. Ikeda, S. Fujimoto, N. Kawakami, and Y. Yanase for valuable discussions. This work is supported by JSPS/MEXT KAKENHI Grant Number 26800177 (Y. T.). RP thanks RIKEN for support through its FPR Program.

-
- * tada@issp.u-tokyo.ac.jp
- ¹ H. Shishido, T. Shibauchi, K. Yasu, T. Kato, H. Kontani, T. Terashima, and Y. Matsuda, *Science* **327**, 980 (2010).
 - ² Y. Mizukami, H. Shishido, T. Shibauchi, M. Shimozaawa, S. Yasumoto, D. Watanabe, M. Yamashita, H. Ikeda, T. Terashima, H. Kontani, et al., *Nat. Phys.* **7**, 849 (2012).
 - ³ S. K. Goh, Y. Mizukami, H. Shishido, D. Watanabe, S. Yasumoto, M. Shimozaawa, M. Yamashita, T. Terashima, Y. Yanase, T. Shibauchi, et al., *Phys. Rev. Lett.* **109**, 157006 (2012).
 - ⁴ M. Shimozaawa, S. K. Goh, R. Endo, R. Kobayashi, T. Watashige, Y. Mizukami, H. Ikeda, H. Shishido, Y. Yanase, T. Terashima, et al., *Phys. Rev. Lett.* **112**, 156404 (2014).
 - ⁵ T. Shinjo, *Introduction to Artificial Lattices* (Uchida Roukakuho Publishing, Tokyo, 2002), (in Japanese).
 - ⁶ L. L. Chang and B. C. Giessen, *Synthetic Modulated Structures* (Academic Press, London, 1985).
 - ⁷ B. Y. Jin and J. B. Ketterson, *Adv. Phys.* **38**, 189 (1989).
 - ⁸ I. Banerjee and I. K. Schuller, *J. Low Temp. Phys.* **54**, 501 (1984).
 - ⁹ K. Kanoda, H. Mazaki, T. Yamada, N. Hosoi, and T. Shinjo, *Phys. Rev. B* **33**, 2052(R) (1986).
 - ¹⁰ P. Grünberg, R. Schreiber, Y. Pang, M. B. Brodsky, and H. Sowers, *Phys. Rev. Lett.* **57**, 2442 (1986).
 - ¹¹ S. S. P. Parkin, N. More, and K. P. Roche, *Phys. Rev. Lett.* **64**, 2304 (1990).
 - ¹² S. S. P. Parkin, *Phys. Rev. Lett.* **67**, 3598 (1991).
 - ¹³ Y. Yafet, *Phys. Rev. B* **36**, 3948 (1987).
 - ¹⁴ P. Bruno, *Phys. Rev. B* **52**, 411 (1995).
 - ¹⁵ J. M. Lawrence and S. M. Shapiro, *Phys. Rev. B* **22**, 4379 (1980).
 - ¹⁶ G. Knebel, D. Braithwaite, P. C. Canfield, G. Lapertot, and J. Flouquet, *Phys. Rev. B* **65**, 024425 (2001).
 - ¹⁷ C. Pfleiderer, *Rev. Mod. Phys.* **81**, 1551 (2009).
 - ¹⁸ C. Petrovic, P. G. Pagliuso, M. F. Hundley, R. Movshovich, J. L. Sarrao, J. D. Thompson, Z. Fisk, and P. Monthoux, *J. Phys. Condens. Matter* **13**, L337 (2001).
 - ¹⁹ C. Stock, C. Broholm, J. Hudis, H. J. Kang, and C. Petrovic, *Phys. Rev. Lett.* **100**, 087001 (2008).
 - ²⁰ Y. Kawasaki, S. Kawasaki, M. Yashima, T. Mito, G. Q. Zheng, Y. Kitaoka, H. Shishido, R. Settai, Y. Haga, and Y. Ōnuki, *J. Phys. Soc. Jpn.* **72**, 2308 (2003).
 - ²¹ H. Shishido, R. Settai, D. Aoki, S. Ikeda, H. Nakawaki, N. Nakamura, T. Iizuka, Y. Inada, K. Sugiyama, T. Takeuchi, et al., *J. Phys. Soc. Jpn.* **71**, 162 (2002).
 - ²² D. Maruyama, M. Sigrist, and Y. Yanase, *J. Phys. Soc. Jpn.* **81**, 034702 (2012).
 - ²³ T. Yoshida, M. Sigrist, and Y. Yanase, *J. Phys. Soc. Jpn.* **82**, 074714 (2013).
 - ²⁴ D. Maruyama, M. Sigrist, and Y. Yanase, *J. Phys. Soc. Jpn.* **82**, 043703 (2012).
 - ²⁵ T. Yoshida, M. Sigrist, and Y. Yanase, *J. Phys. Soc. Jpn.* **83**, 013703 (2014).
 - ²⁶ J. H. She and A. V. Balatsky, *Phys. Rev. Lett.* **109**, 077002 (2012).
 - ²⁷ Y. Tada, R. Peters, and M. Oshikawa, *Phys. Rev. B* **88**, 235121 (2013).
 - ²⁸ R. Peters, Y. Tada, and N. Kawakami, *Phys. Rev. B* **88**, 155134 (2013).
 - ²⁹ Y. Yanase, T. Jujo, T. Nomura, H. Ikeda, T. Hotta, and K. Yamada, *Phys. Rep.* **387**, 1 (2003).
 - ³⁰ In preparation.
 - ³¹ P. G. de Gennes and E. Guyon, *Phys. Lett.* **3**, 168 (1963).
 - ³² P. G. de Gennes, *Rev. Mod. Phys.* **36**, 225 (1964).
 - ³³ N. R. Werthamer, *Phys. Rev.* **132**, 2440 (1963).
 - ³⁴ J. J. Hauser, H. C. Theuerer, and N. R. Werthamer, *Phys. Rev.* **136**, A637 (1964).
 - ³⁵ P. Monthoux and G. G. Lonzarich, *Phys. Rev. B* **63**, 054529 (2001).
 - ³⁶ R. Arita, K. Kuroki, and H. Aoki, *J. Phys. Soc. Jpn.* **69**, 1181 (2000).